Digital Monopulse Beamforming for Achieving the CRLB for Angle Accuracy

RYUHEI TAKAHASHI , Member, IEEE
TAKAYUKI INABA, Senior Member, IEEE
TORU TAKAHASHI, Senior Member, IEEE
HIROHISA TASAKI
Mitsubishi Electric Corporation, Kamakura, Japan, and University of Electro-Communications, Tokyo, Japan

The monopulse angle-estimation technique used in digital beamforming radars is investigated from the perspective of optimizing the angle accuracy. Specifically, a digital difference beamforming taper is proposed in this paper to optimize the monopulse angle accuracy. For a fully digitized array radar with an amplitude-tapered antenna aperture for sum beampattern with low sidelobes, the monopulse angle accuracy obtained using the proposed difference taper coincides with the Cramer–Rao lower bound. The derivation of the monopulse angle accuracy with the proposed difference taper is presented and an improvement of the accuracy over the conventional monopulse accuracy is proved theoretically. The results of computer simulations using a uniform linear array is included to highlight the accuracy improvement by a factor of 1.16 (over the conventional monopulse), which is equivalent to a 1.3 dB reduction in the signal-to-noise ratio for the requisite angle accuracy.

Manuscript received August 20, 2016; revised April 25, 2017; released for publication July 31, 2017. Date of publication September 26, 2017; date of current version February 7, 2018.

DOI. No. 10.1109/TAES.2017.2756519

Refereeing of this contribution was handled by R. S. Raghavan.

Authors' addresses: R. Takahashi is with the Information Technology R&D Center, Mitsubishi Electric Corporation, Kamakura, Japan, and also with the Graduate School of Informatics and Engineering, University of Electro-Communications, Tokyo 182-8585, Japan, E-mail: (Takahashi.Ryuhei@ab.MitsubishiElectric.co.jp); T. Inaba is with the Graduate School of Informatics and Engineering, University of Electro-Communications, Tokyo 182-8585, Japan, E-mail: (inaba@ee.uec.ac.jp); T. Takahashi and H. Tasaki are with the Information Technology R&D Center, Mitsubishi Electric Corporation, Kamakura 247-8501, Japan. E-mail: (Takahashi.Toru@dx.MitsubishiElectric.co.jp; Tasaki.Hirohisa@dx.MitsubishiElectric.co.jp). *(Corresponding author: Ryuhei Takahashi).*

0018-9251 © 2017 IEEE

NOMENCLATURE

$\mathbf{a}(u)$	Steering vector for angle u in sine space.
$\mathbf{a}'(u)$	$= \mathbf{T}_{\mathrm{SL}}\mathbf{a}(u)$. Steering vector after amplitude taper.
BW	Sum beamwidth.
d_m	The mth element antenna position originating from the antenna center.
$\mathbf{D}$	Diagonal matrix given by $\mathbf{D} = \mathrm{diag}(d_1, d_2, \ldots, d_M)$.
ESNR	Signal-to-noise power ratio at an element antenna.
$\mathbf{I}$	Identity matrix.
$\mathbf{J}$	Fisher's information matrix (FIM).
$k^{(\mathrm{dg})}$	Degradation factor of the monopulse angle accuracy.
$km^{(\mathrm{cnv})}$	Normalized monopulse slope for a conventional monopulse.
$km^{(\mathrm{opt})}$	Normalized monopulse slope for an optimum monopulse.
L_{SNR}	Gain loss due to the amplitude taper for sum beamforming.
$\mathbf{n}(t)$	White Gaussian receiver noise vector.
$\mathbf{n}'(t)$	$= \mathbf{T}_{SL}\mathbf{n}(t)$. Receiver noise vector after amplitude taper.
p_s	Signal power.
SNR	Signal-to-noise power ratio after sum beamforming and slow-time coherent integration.
$s(t)$	Complex amplitude of the target signal.
t	Snapshot index.
T	Number of snapshots.
$\mathbf{T}_{\mathrm{SL}}$	Amplitude-taper matrix.
$\mathbf{w}_\Delta$	Optimum difference taper.
$\mathbf{w}_\Delta^{(\mathrm{cnv})}$	Conventional difference taper.
$\mathbf{w}_\Sigma$	Sum beamforming weight.
$\mathbf{x}(t)$	Received vector.
α_m	Amplitude-taper coefficients for the sum beampattern.
λ	Wavelength.
$\boldsymbol{\theta}$	Unknown parameter vector.
σ^2	Average power of the white Gaussian receiver noise.
$\sigma^{(\mathrm{cnv})}$	Conventional monopulse angle accuracy.
$\sigma^{(\mathrm{CRLB})}$	$= \sigma^{(\mathrm{CRLB})}(0)$. CRLB for angle accuracy for an on-boresight target.
$\sigma^{(\mathrm{CRLB})}(u)$	CRLB for angle accuracy.
$\sigma^{(\mathrm{opt})}$	Optimum monopulse angle accuracy.
$\Lambda(\boldsymbol{\theta})$	Likelihood function for $\boldsymbol{\theta}$.

I. INTRODUCTION

Monopulse angle-estimation technique, or simply "monopulse," has been used in a wide range of radar systems to determine the angular location of a tracking target [1]–[3]. In monopulse, the sum and difference beams are formed simultaneously to estimate the direction of arrival (DOA) of the target within the sum beamwidth. In a conventional phased array radar in which the antenna aperture is typically amplitude-tapered for the lower sidelobes of the sum beampattern, the outputs of the symmetrically divided left and right (or upper and lower) quadrants of the aperture are used to form the sum and difference beams with a monopulse comparator network [3]. The sum beam with lower sidelobes is formed by adding all the quadrant outputs and the azimuth difference beam is formed by subtracting the left quadrant output from the right quadrant output. In a similar manner, the elevation difference beam is formed using the upper and lower quadrant outputs. With the monopulse comparator, the difference beampattern is determined uniquely from the aperture design for the sum beampattern; it cannot be designed independent from the sum beampattern.[1]

The monopulse angle accuracy is derived from the root-mean-square error (RMSE) of the measured monopulse ratio and is given by the signal-to-noise power ratio (SNR), the 3 dB beamwidth of the sum mainbeam, and the normalized monopulse slope [1]–[3].[2] The monopulse angle accuracy can be designed to meet the requisite angle accuracy by careful design of these three parameters. Clearly, the sum beamwidth and SNR are affected by the antenna aperture design for the sum beampattern while the normalized monopulse slope is determined by the sum beampattern as well as by the difference beampattern. Thus, if the sum beampattern is to be maintained constant (to maintain the radar detection sensitivity), only the difference beampattern will have an impact on the monopulse angle-accuracy improvement through monopulse slope design. However, as mentioned earlier, it is not possible to design the difference beampattern independently in conventional phased array radars. Hence, the monopulse angle accuracy is uniquely determined by the aperture design for the sum beampattern because the design of a normalized monopulse slope is unrealized.

Recent advanced phased array radar systems employ digital beamforming (DBF) in place of the monopulse comparator network to form the analog sum and difference beams. DBF allows digital monopulse beamforming so that a flexible azimuth and/or elevation difference beamforming, which is independent from the sum beamforming, can be achieved. This gives a certain degree of freedom in the design of the monopulse angle accuracy, unlike in conventional phased array radars, and makes it possible to improve the accuracy to achieve the Cramer–Rao lower bound (CRLB), which provides a lower bound for the angle accuracy of an unbiased estimator.

The CRLB for angle accuracy for a single target impinging on an array antenna has been studied in some literatures [8]–[10]. In the development of the CRLB, in those literatures, a steering vector for the target direction and its derivative vector with respect to the direction cosine are introduced; these are often called the "sum" and "difference" filters [9], namely, the sum and difference tapers, in array signal processing context. These steering vectors are also used in the closed form for estimating the DOA of a single target in the generalized monopulse angle estimation [3] and the maximum likelihood estimator [11], which is a DOA-estimation technique to achieve the CRLB. These reports imply that the monopulse angle accuracy could reach the CRLB by applying the sum and difference tapers in the DBF process. In [12], the CRLB is compared with the CRLB for monopulse processing using a pair of sum beams formed from an array output.

To the authors' knowledge, there are no open literatures (including [1]–[12]) that discuss the theoretical and quantitative relationship between the monopulse angle accuracy for conventional phased array radar and the CRLB for angle accuracy.[3] In this regard, we compare the conventional monopulse angle accuracy with the CRLB theoretically and quantify the potential improvement of the monopulse angle accuracy in a fully digitized array radar. The improvement is given by (25). Subsequently, the optimum difference taper is proposed to achieve the CRLB by digital monopulse beamforming. Specifically, a linear relational expression is derived by equating the formula for monopulse angle accuracy with the CRLB for angle accuracy. The optimum difference taper is obtained by solving a constrained optimization problem where the relational expression is used as single linear constraint. The solution given by (35) reveals that the optimum difference taper is the same as the derivative of the sum beampattern. It should be noted that the optimum difference taper is obtained without any changes in the sum beampattern, to maintain target detection sensitivity.

The remainder of this paper is organized as follows: In Section II, the general CRLB for angle accuracy for a single target impinging on a linear array antenna is briefly presented. By considering the symmetrical element antenna arrangement about the antenna center in monopulse beamforming, and the target location using the boresight in the tracking mode, the CRLB studied in this paper is derived from the general CRLB. In Section III, the CRLB given in Section II and the conventional monopulse angle accuracy are theoretically compared and the improvement in the monopulse angle accuracy in fully digitized array radars is quantified. In Section IV, an optimum difference taper is proposed to achieve CRLB with digital monopulse beamforming. In Section V, the results of computer simulations are presented to show that the monopulse using the optimum difference taper can achieve an angle accuracy that coincides with the CRLB for angle accuracy. The concluding remarks for this study are provided in Section VI.

[1]There are phased array architectures that enable independent control of the sum and difference beampatterns [4]. These are, however, expensive and complex to implement in practice.

[2]The accuracy is valid for the case in which a single target interfered with receiver noise is received. Some studies address monopulse angle accuracy under a jamming or unresolved targets scenario [5]–[7]. This study is limited to the former case.

[3]The works in [13] and [14] by R. Takahashi are exceptions. In those papers, an optimum difference taper to achieve the CRLB for angle accuracy has been presented without the derivation. The derivation of the optimum difference taper is described in detail in this paper.

II. CRLB FOR ANGLE ACCURACY

A. FIM and CRLB for Angle Accuracy for Linear Arrays

Let us consider a signal model for a single target arriving at a tapered linear array antenna. A linear array antenna is used in this paper for simplifying the discussion; moreover, extension of this study to the planar array antenna becomes straightforward. The received vector $\mathbf{x}(t)$ for an M-element array and the snapshot index t with a total of T snapshots is given as

$$\begin{aligned}\mathbf{x}(t) &= \mathbf{T}_{\mathrm{SL}}\left(\mathbf{a}(u)s(t)+\mathbf{n}(t)\right)\\ &= \mathbf{a}'(u)s(t)+\mathbf{n}'(t).\end{aligned} \tag{1}$$

where $s(t)$ is the complex amplitude of the target signal and $\mathbf{n}(t)$ is the white Gaussian receiver noise vector with average power σ^2. $\mathbf{T}_{\mathrm{SL}}$ is a real-valued amplitude-taper matrix whose diagonal components are amplitude-taper coefficients α_m, for achieving lower antenna sidelobes in the sum beampattern. Specifically, $\mathbf{T}_{\mathrm{SL}}$ is given as

$$\mathbf{T}_{\mathrm{SL}} = \mathrm{diag}\left(\alpha_1, \ldots, \alpha_M\right). \tag{2}$$

$\mathbf{a}(u)$ is a steering vector for a target angle u in sine space and is given as

$$\mathbf{a}(u) = \left[\exp\left(j\frac{2\pi d_1}{\lambda}u\right), \ldots, \exp\left(j\frac{2\pi d_M}{\lambda}u\right)\right]^T \tag{3}$$

where d_m is the mth element antenna position on the linear array originating from the antenna center and λ is the wavelength. $\mathbf{a}'(u)$ and $\mathbf{n}'(t)$ are steering vectors for the target angle u and receiver noise vector after amplitude tapering with $\mathbf{T}_{\mathrm{SL}}$, respectively, and are given as

$$\mathbf{a}'(u) = \mathbf{T}_{\mathrm{SL}}\mathbf{a}(u), \tag{4}$$

$$\mathbf{n}'(t) = \mathbf{T}_{\mathrm{SL}}\mathbf{n}(t). \tag{5}$$

The FIM $\mathbf{J}$ is defined as [15]

$$[\mathbf{J}]_{ij} = J_{ij} \equiv E\left[\frac{\partial \ln \Lambda(\theta)}{\partial \theta_i}\frac{\partial \ln \Lambda(\theta)}{\partial \theta_j}\right] \tag{6}$$

where $i = 1, ..., 2T+2$ and $j = 1, ..., 2T+2$ are the index numbers, and θ is a parameter vector containing $2T+2$ unknown parameters in the signal model in (1) given by $\theta = [u, \sigma, \mathrm{Re}(s(1)), \mathrm{Im}(s(1)), ..., \mathrm{Re}(s(T)), \mathrm{Im}(s(T))]^T$. $\Lambda(\theta)$ is the likelihood function for θ.

The CRLB provides a lower bound on the performance of an unbiased estimator. It is obtained by solving the diagonal elements of the inverse of the FIM given in (6). The derivation of the CRLB for a target signal impinging on a linear array at an angle u is straightforward as shown in [15]. The CRLB for angle accuracy $\sigma^{(\mathrm{CRLB})}(u)$ is given by

$$\sigma^{(\mathrm{CRLB})}(u) = \frac{\lambda}{2\pi}\sqrt{\frac{1}{2T\cdot\mathrm{ESNR}}\left[\mathbf{a}^H(u)\mathbf{DPDa}(u)\right]^{-1}} \tag{7}$$

where ESNR is the signal-to-noise power ratio at an element antenna and is given by

$$\mathrm{ESNR} = \frac{p_s}{\sigma^2} \tag{8}$$

where p_s is the signal power, and matrix $\mathbf{P}$ is given by

$$\mathbf{P} = \mathbf{I} - \frac{\mathbf{a}(u)\mathbf{a}^H(u)}{\mathbf{a}(u)^H\mathbf{a}(u)} \tag{9}$$

where $\mathbf{D}$ is the diagonal matrix given by $\mathbf{D} = \mathrm{diag}(d_1, d_2, ..., d_M)$.

B. CRLB for Angle Accuracy for On-Boresight Target With Symmetrical Linear Array

To realize monopulse angle estimation in a phased array radar, the antenna elements should be positioned in a symmetric fashion around the antenna center. Specifically, the antenna aperture of the M-element linear array should be divided into two quadrants with $M/2$ elements each. The element antenna positions d_m in this arrangement can be expressed as

$$\begin{aligned}&\left\{d_1, d_2, ..., d_{\frac{M}{2}}, d_{\frac{M}{2}+1}, ..., d_{M-1}, d_M\right\}\\ &= \left\{d_1, d_2, ..., d_{\frac{M}{2}}, -d_{\frac{M}{2}}, ..., -d_2, -d_1\right\}.\end{aligned} \tag{10}$$

The amplitude-taper coefficient α_m for the sum beamforming is expressed in response to the symmetrical arrangement of the element antenna positions as

$$\begin{aligned}&\left\{\alpha_1, \alpha_2, ..., \alpha_{\frac{M}{2}}, \alpha_{\frac{M}{2}+1}, ..., \alpha_{M-1}, \alpha_M\right\}\\ &= \left\{\alpha_1, \alpha_2, ..., \alpha_{\frac{M}{2}}, \alpha_{\frac{M}{2}}, ..., \alpha_2, \alpha_1\right\}.\end{aligned} \tag{11}$$

The detailed derivations of the CRLB for the symmetrical linear array are provided in the Appendix. The CRLB for angle accuracy $\sigma^{(\mathrm{CRLB})}(u)$ is reduced from (7) to

$$\sigma^{(\mathrm{CRLB})}(u) = \frac{\lambda}{2\pi}\sqrt{\frac{1}{2T\cdot\mathrm{ESNR}}\left[\mathbf{a}^H(u)\mathbf{DDa}(u)\right]^{-1}}. \tag{12}$$

We now consider the case of $u = 0$, i.e., a target is located at the antenna boresight in the tracking mode. In this case, the CRLB for angle accuracy for an on-boresight target with a symmetrical linear array, now termed $\sigma^{(\mathrm{CRLB})}$, is further reduced from (12) to

$$\sigma^{(\mathrm{CRLB})} = \frac{\lambda}{4\pi}\frac{1}{\sqrt{T\cdot\mathrm{ESNR}\cdot\sum_{m=1}^{M/2}{d_m}^2}}. \tag{13}$$

III. CRLB AND CONVENTIONAL MONOPULSE ANGLE ACCURACY

In this section, the conventional monopulse angle accuracy is presented and is manipulated to express with the CRLB given by (13). Because the amplitude-taper coefficients α_m for the lower sidelobes sum beampattern is applied in the antenna aperture as seen in (1), the digital weight $\mathbf{w}_\Sigma$ for sum beamforming in a fully digitized array radar is given as

$$\mathbf{w}_\Sigma = \mathbf{1}_{M\times 1} \tag{14}$$

where $\mathbf{1}_{M\times 1}$ is a $M \times 1$ dimensional all-one vector.

In response to the difference beamforming with a monopulse comparator in conventional phased array radars, the equivalent conventional difference taper $\mathbf{w}_{\Delta}^{(\mathrm{cnv})}$ for DBF can be expressed as

$$\mathbf{w}_{\Delta}^{(\mathrm{cnv})} = \left[+1 \cdots +1 -1 \cdots -1\right]^{T}. \tag{15}$$

Clearly, $\mathbf{w}_{\Sigma}$ and $\mathbf{w}_{\Delta}^{(\mathrm{cnv})}$ are orthogonal, i.e., ${\mathbf{w}_{\Sigma}}^{H}\mathbf{w}_{\Delta}^{(\mathrm{cnv})} = 0$. The monopulse error function for u close to the antenna boresight, i.e., $u \leftarrow 0$ is approximated by a linear function [2] as

$$\frac{km^{(\mathrm{cnv})}}{\mathrm{BW}} u = \mathrm{Im}\left(\frac{{\mathbf{w}_{\Delta}^{(\mathrm{cnv})}}^{H}\mathbf{a}'(u)}{{\mathbf{w}_{\Sigma}}^{H}\mathbf{a}'(u)}\right) \tag{16}$$

where $km^{(\mathrm{cnv})}$ is the normalized monopulse slope for a conventional monopulse and BW is the sum beamwidth. This function is used as a reference to transfer the measured monopulse ratio into the off-boresight angle, namely, the target angle u. Note that the measured monopulse ratio is the imaginary part of the difference-beam output to the sum-beam output ratio, and it corresponds to the right-hand side of (16).

From (10), (11), and (15), ${\mathbf{w}_{\Sigma}}^{H}\mathbf{a}'(u)$ and $\mathbf{w}_{\Delta}^{(\mathrm{cnv})\mathrm{H}}\mathbf{a}'(u)$ in (16) are reduced, respectively, to

$${\mathbf{w}_{\Sigma}}^{H}\mathbf{a}'(u) = 2\sum_{m=1}^{M/2}\alpha_m \tag{17}$$

$${\mathbf{w}_{\Delta}^{(\mathrm{cnv})}}^{H}\mathbf{a}'(u) = j\frac{4\pi}{\lambda}\left(\sum_{m=1}^{M/2}\alpha_m d_m\right)u. \tag{18}$$

Substituting (17) and (18) into (16), $km^{(\mathrm{cnv})}$ is expressed as

$$km^{(\mathrm{cnv})} = \mathrm{BW}\frac{2\pi}{\lambda}\frac{\sum_{m=1}^{M/2}\alpha_m d_m}{\sum_{m=1}^{M/2}\alpha_m}. \tag{19}$$

The conventional monopulse angle accuracy for an on-boresight target $\sigma^{(\mathrm{cnv})}$ is derived from the RMSE of the measured monopulse ratio and is expressed as [2]

$$\sigma^{(\mathrm{cnv})} = \frac{\mathrm{BW}}{km^{(\mathrm{cnv})}}\frac{1}{\sqrt{2\mathrm{SNR}}} \tag{20}$$

where SNR is the signal-to-noise power ratio after sum beamforming and slow-time coherent integration with T snapshot. It is expressed as

$$\mathrm{SNR} = L_{\mathrm{SNR}} \cdot T \cdot M \cdot \mathrm{ESNR} \tag{21}$$

where L_{SNR} is the gain loss due to the amplitude taper for sum beamforming. Note that the gain loss due to the slow-time coherent integration has been discarded for simplifying the discussion. By substituting (19) and (21) into (20), $\sigma^{(\mathrm{cnv})}$ can be expressed as

$$\sigma^{(\mathrm{cnv})} = \frac{\lambda}{2\pi}\frac{\sum_{m=1}^{M/2}\alpha_m}{\sum_{m=1}^{M/2}\alpha_m d_m}\frac{1}{\sqrt{2L_{\mathrm{SNR}}TM \cdot \mathrm{ESNR}}}. \tag{22}$$

To express (22) with $\sigma^{(\mathrm{CRLB})}$ in (13), it should be noted that L_{SNR} [16] is given as

$$L_{\mathrm{SNR}} = \frac{2\left(\sum_{m=1}^{M/2}\alpha_m\right)^2}{M\sum_{m=1}^{M/2}{\alpha_m}^2} \tag{23}$$

by considering the symmetrical arrangement in (10). By substituting (23) into (22), the conventional monopulse angle accuracy $\sigma^{(\mathrm{cnv})}$ can be finally expressed with the $\sigma^{(\mathrm{CRLB})}$ in (13) as

$$\sigma^{(\mathrm{cnv})} = k^{(\mathrm{dg})}\sigma^{(\mathrm{CRLB})} \tag{24}$$

where $k^{(\mathrm{dg})}$ is the degradation factor of the conventional monopulse angle accuracy $\sigma^{(\mathrm{cnv})}$ with respect to $\sigma^{(\mathrm{CRLB})}$, and is given by

$$k^{(\mathrm{dg})} = \frac{\sqrt{\sum_{m=1}^{M/2}{\alpha_m}^2}\sqrt{\sum_{m=1}^{M/2}{d_m}^2}}{\sum_{m=1}^{M/2}\alpha_m d_m}. \tag{25}$$

It should be noted that $k^{(\mathrm{dg})} \geq 1$ is guaranteed by the Cauchy–Schwarz inequality and $k^{(\mathrm{dg})} = 1$ is satisfied only when $M = 2$. In general, $M > 2$ holds for typical phased array radars with plenty of element antennas; therefore, $k^{(\mathrm{dg})} > 1$ will hold in practice.

From (24), it can be concluded that the conventional monopulse angle accuracy $\sigma^{(\mathrm{cnv})}$ is generally not optimum from the point of view of maximizing the angle accuracy. Degradation of the accuracy with respect to CRLB can be quantified by introducing the degradation factor $k^{(\mathrm{dg})}$ given by (25). A quantitative discussion on $k^{(\mathrm{dg})}$ is given in the next section.

IV. MONOPULSE DIFFERENCE BEAMFORMING ACHIEVING CRLB

A. Optimum Difference Taper

In a fully digitized array radar, independent and flexible difference beamformings are available from the sum beamforming. The optimum difference taper to achieve the CRLB for angle accuracy, through a combination with an arbitrary sum beamforming, is proposed in this section. The sum weight $\mathbf{w}_{\Sigma}$ is unchanged for the lower sidelobes in the sum beampattern, and the optimum difference taper to improve the monopulse angle accuracy to the CRLB is termed as $\mathbf{w}_{\Delta}$, where

$$\mathbf{w}_{\Delta} = \left[+w_1, +w_2, ..., +w_{\frac{M}{2}}, -w_{\frac{M}{2}}, ..., -w_2, -w_1\right]^{T}. \tag{26}$$

The monopulse error function with $\mathbf{w}_{\Sigma}$ and $\mathbf{w}_{\Delta}$ beamformers is given as

$$\frac{km^{(\mathrm{opt})}}{\mathrm{BW}} u = \mathrm{Im}\left(\frac{{\mathbf{w}_{\Delta}}^{H}\mathbf{a}'(u)}{{\mathbf{w}_{\Sigma}}^{H}\mathbf{a}'(u)}\right) \tag{27}$$

where $km^{(\mathrm{opt})}$ is the normalized monopulse slope from the optimum monopulse beamformers $\mathbf{w}_{\Sigma}$ and $\mathbf{w}_{\Delta}$. By differentiating (27) with respect to u, $km^{(\mathrm{opt})}$ can be expressed as

$$km^{(\text{opt})} = \text{BW}\frac{\partial}{\partial u}\text{Im}\left(\frac{\mathbf{w}_\Delta{}^H\mathbf{a}'(u)}{\mathbf{w}_\Sigma{}^H\mathbf{a}'(u)}\right). \tag{28}$$

Thus, the angle accuracy $\sigma^{(\text{opt})}$ by the optimum monopulse beamformer is given as

$$\begin{aligned}\sigma^{(\text{opt})} &= \frac{\text{BW}}{km^{(\text{opt})}\sqrt{2\text{SNR}}}\\ &= \frac{1}{\frac{\partial}{\partial u}\text{Im}\left(\frac{\mathbf{w}_\Delta{}^H\mathbf{a}'(u)}{\mathbf{w}_\Sigma{}^H\mathbf{a}'(u)}\right)\sqrt{2\text{SNR}}}.\end{aligned} \tag{29}$$

Since the optimum difference taper $\mathbf{w}_\Delta$ is introduced to achieve the CRLB for angle accuracy, (13) and (29) should be equal so that the following equation is satisfied:

$$\frac{1}{\frac{\partial}{\partial u}\text{Im}\left(\frac{\mathbf{w}_\Delta{}^H\mathbf{a}'(u)}{\mathbf{w}_\Sigma{}^H\mathbf{a}'(u)}\right)\sqrt{2\text{SNR}}} = \frac{\lambda}{4\pi}\frac{1}{\sqrt{T\cdot\text{ESNR}\cdot\sum_{m=1}^{M/2}d_m{}^2}}. \tag{30}$$

$\mathbf{w}_\Delta{}^H\mathbf{a}'(u)$ in (30) is reduced as

$$\mathbf{w}_\Delta{}^H\mathbf{a}'(u) = j\frac{4\pi}{\lambda}\left(\sum_{m=1}^{M/2} w_m{}^*\alpha_m d_m\right)u. \tag{31}$$

By substituting (17) and (31), (30) is manipulated to the following relational expression:

$$\sum_{m=1}^{M} w_m{}^*\alpha_m d_m = \sqrt{\sum_{m=1}^{M} d_m{}^2}\sqrt{\sum_{m=1}^{M}\alpha_m{}^2}. \tag{32}$$

By expressing the left-hand side of (32) in vector and matrix forms, the following linear combination for $\mathbf{w}_\Delta$ to achieve the CRLB is finally derived

$$\mathbf{w}_\Delta{}^H\mathbf{T}_{\text{SL}}\text{diag}(\mathbf{D}) = \sqrt{\sum_{m=1}^{M}\alpha_m{}^2\sum_{m=1}^{M} d_m{}^2}. \tag{33}$$

To achieve the CRLB for angle accuracy using the optimum monopulse beamformer, a linearly constrained optimization problem for $\mathbf{w}_\Delta$ is formulated as

$$\begin{aligned}&\min\ \mathbf{w}_\Delta{}^H\mathbf{R}_{nn}\mathbf{w}_\Delta\\ &\quad\text{subject to } \mathbf{w}_\Delta{}^H\mathbf{T}_{SL}\text{diag}(\mathbf{D}) = \sqrt{\sum_{m=1}^{M}\alpha_m{}^2\sum_{m=1}^{M}d_m{}^2}.\end{aligned} \tag{34}$$

Equation (33) is used as a single linear constraint in this optimization problem. $\mathbf{w}_\Delta$ in (34) is solved in a straightforward manner as

$$\mathbf{w}_\Delta = \sqrt{\frac{\sum_{m=1}^{M}\alpha_m{}^2}{\sum_{m=1}^{M}d_m{}^2}}\mathbf{d}' \tag{35}$$

where

$$\begin{aligned}\mathbf{d}' &= \mathbf{T}_{\text{SL}}^{-1}\text{diag}(\mathbf{D})\\ &= \left[\frac{d_1}{\alpha_1},\ldots,\frac{d_{\frac{M}{2}}}{\alpha_{\frac{M}{2}}},-\frac{d_{\frac{M}{2}}}{\alpha_{\frac{M}{2}}},\ldots,-\frac{d_1}{\alpha_1}\right]^T.\end{aligned} \tag{36}$$

The optimum difference taper $\mathbf{w}_\Delta$ is now obtained with a scale factor $\sqrt{\sum_{m=1}^{M}\alpha_m{}^2/\sum_{m=1}^{M}d_m{}^2}$ and vector $\mathbf{d}'$. It is clear that $\mathbf{d}'$ applies the element antenna position d_m as a taper weight while cancelling the amplitude-taper coefficient α_m for sum beamforming. $\mathbf{w}_\Sigma$ and $\mathbf{w}_\Delta$ are orthogonal, i.e., $\mathbf{w}_\Sigma{}^H\mathbf{w}_\Delta = 0$.

To confirm that the optimum monopulse beamformer with $\mathbf{w}_\Sigma$ and $\mathbf{w}_\Delta$ can achieve the CRLB for angle accuracy, (35) is substituted into (31) as

$$\mathbf{w}_\Delta{}^H\mathbf{a}'(u) = j\frac{4\pi}{\lambda}\sqrt{\sum_{m=1}^{M/2}\alpha_m{}^2\sum_{m=1}^{M/2}d_m{}^2}u. \tag{37}$$

Substituting (17) and (37) into (28), the normalized monopulse slope for the optimum monopulse beamformer can be obtained as

$$km^{(\text{opt})} = \text{BW}\frac{2\pi}{\lambda}\frac{\sqrt{2\sum_{m=1}^{M/2}d_m{}^2}}{\sqrt{L_{\text{SNR}}M}}. \tag{38}$$

Thus, the monopulse angle accuracy can be rewritten as

$$\sigma^{(\text{opt})} = \frac{\lambda}{4\pi}\frac{1}{\sqrt{T\cdot\text{ESNR}\cdot\sum_{m=1}^{M/2}d_m{}^2}}. \tag{39}$$

It is clearly confirmed that the monopulse angle accuracy in (39) is in agreement with the CRLB for angle accuracy derived by (13), namely $\sigma^{(\text{opt})} = \sigma^{(\text{CRLB})}$. Hence, the monopulse angle estimation with the proposed optimum difference taper $\mathbf{w}_\Delta$ can achieve the CRLB for angle accuracy.

Subarray-based DBF with several tens of channels is a practical solution for phased array radars with hundreds or thousands of antenna elements [3]. For this case, the suboptimum difference beamforming taper can be derived with respect to the optimum difference beamforming taper $\mathbf{w}_\Delta$[13].

B. Monopulse Angle-Accuracy Improvement

A theoretical comparison between the optimum and conventional monopulse estimations is performed. From (24), the angle accuracy with the optimum difference taper is given as

$$\sigma^{(\text{opt})} = \frac{1}{k^{(\text{dg})}}\sigma^{(\text{cnv})}. \tag{40}$$

Thus, the angle accuracy with optimum difference taper is improved by a factor of $1/k^{(\text{dg})}$ with respect to the conventional monopulse angle accuracy. If the requisite angle accuracy is specified as $\sigma^{(\text{req})}$, the SNR to meet the requisite accuracy by the conventional monopulse is obtained from (40) as

$$\text{SNR}_0^{(\text{cnv})} = \frac{1}{2}\left(\frac{k^{(\text{dg})}\text{BW}}{km^{(\text{opt})}\sigma^{(\text{cnv})}}\right)^2. \tag{41}$$

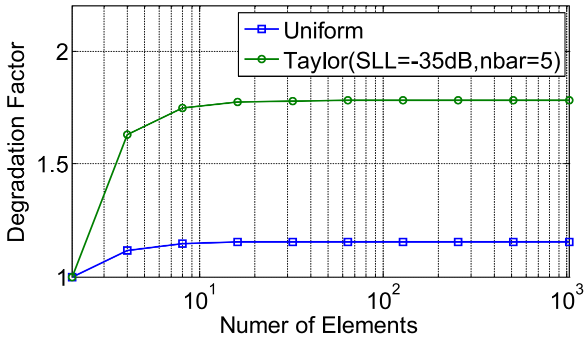

Fig. 1. Degradation factor for different amplitude taper.

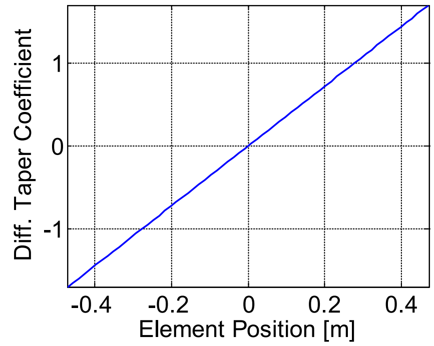

Fig. 2. Difference tapers for fully digitized 64-element ULA.

For an optimum monopulse, the SNR to meet the requisite accuracy $\mathrm{SNR}_0^{(\mathrm{opt})}$ is obtained from (29) as

$$\mathrm{SNR}_0^{(\mathrm{opt})} = \frac{1}{2}\left(\frac{\mathrm{BW}}{km^{(\mathrm{opt})}\sigma^{(\mathrm{cnv})}}\right)^2. \tag{42}$$

Thus, the following expression is derived from (41) and (42)

$$\mathrm{SNR}_0^{(\mathrm{opt})} = \left(\frac{1}{k^{(\mathrm{dg})}}\right)^2 \mathrm{SNR}_0^{(\mathrm{cnv})}. \tag{43}$$

Equation (43) reveals that the requisite SNR for the optimum monopulse is reduced by a factor of $(1/k^{(\mathrm{dg})})^2$ with respect to the conventional monopulse. This means that the radar system could allocate a smaller SNR and time-on-target to track the radar target with the requisite accuracy and thus, could increase the search efficiency or number of tracking targets.

A specific degradation factor for the uniform linear array (ULA) with uniform taper and Taylor taper with a 35 dB sidelobe level is calculated using (25) and the results are shown in Fig. 1. It is observed that the ULA with the Taylor taper has a larger degradation factor compared to the uniform taper and that both factors are little affected by the number of antenna elements M, if M is larger than 16. For $M = 64$, the degradation factors $k^{(\mathrm{dg})}$ are 1.16 and 1.78 for the uniform and the Taylor taper, respectively. From (43), these values correspond to 1.3 and 5.0 dB of SNR reduction, respectively.

A combination of the Taylor taper and the optimum difference taper should be considered carefully in practical radar design. Sum beamforming with Taylor taper realizes maximum detection sensitivity while minimizing possible sidelobe interferences by lowering the antenna sidelobes. Difference beamforming with the optimum taper is, however, designed to maximize the monopulse angle accuracy without any explicit constraints on the antenna sidelobes and thus, it has higher sidelobes compared to the Taylor beampattern [14]. Difference beamforming with Bayliss taper is known to maximize the monopulse angle accuracy while lowering the antenna sidelobes [17], [18]. Monopulse beamforming with Taylor and Bayliss tapers no longer achieves the CRLB for angle accuracy.

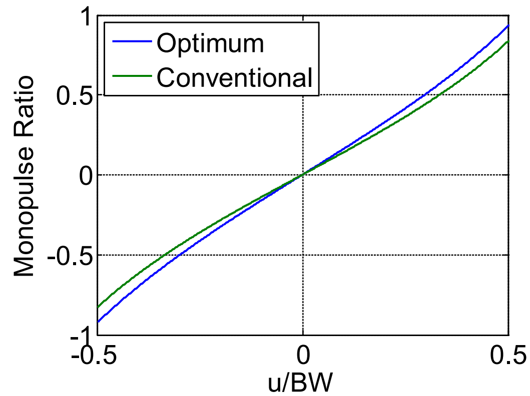

Fig. 3. Monopulse error function for fully digitized 64-element ULA.

V. COMPUTER SIMULATION

Numerical simulations were carried out to validate the angle-accuracy improvement of the monopulse using the proposed optimum difference taper over the conventional monopulse. A scenario in which a single target signal impinges on a ULA consisting of 64 elements with half-wavelength element spacing (where wavelength λ is 0.03 m) was considered. The RMSEs of the estimated angles over 1000 trials were validated for SNRs ranging from 10 to 40 dB. A uniform taper was used for sum beamforming to maximize the detection performance without any special care for lowering the sidelobes.

The proposed optimum taper $\mathbf{w}_\Delta$ from (35) is shown in Fig. 2. Since a uniform taper for sum beamforming is applied, i.e., $\alpha_m = 1$, $\mathbf{w}_\Delta$ is given as a linear function of the antenna-element position d_m. The monopulse error functions for the optimum and conventional monopulses with (15) are shown in Fig. 3. The horizontal axis of Fig. 3 is the direction cosine u normalized by the sum beamwidth. It is observed that the error function for the optimum monopulse has a slightly higher sensitivity for the direction cosine u. The slopes of the error curves, i.e., the normalized monopulse slopes are estimated from the figure as $\widehat{km}^{(\mathrm{opt})} = 1.61$ and $\widehat{km}^{(\mathrm{cnv})} = 1.39$. The estimated coefficient for the optimum monopulse is very close to the theoretical value $km^{(\mathrm{opt})} = 1.60$ obtained from (38). The theoretical value of $km^{(\mathrm{cnv})} = 1.39$ can be obtained by substituting $km^{(\mathrm{opt})} = 1.60$ and $k^{(\mathrm{dg})} = 1.16$ into (40), and it

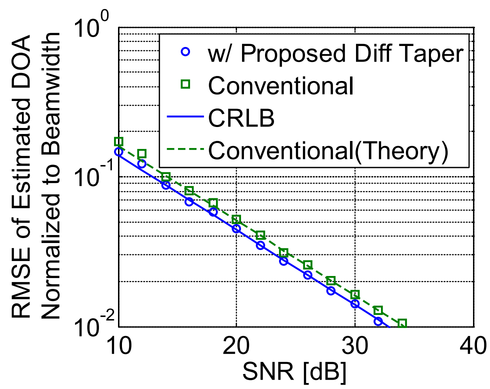

Fig. 4. Monopulse angle accuracy for fully digitized 64-element ULA.

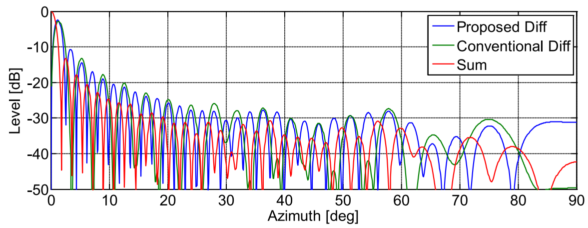

Fig. 5. Monopulse beam patterns for fully digitized 64-element ULA.

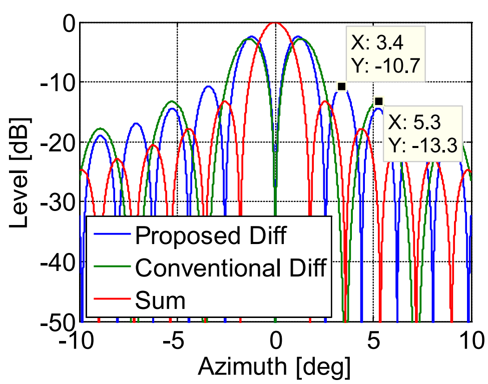

Fig. 6. Zoom of the mainbeam region of Fig. 5.

is in agreement with the estimated value $\widehat{km}^{(\mathrm{cnv})}$. The RMSEs of the SNRs of the monopulses with the proposed and conventional difference tapers—$\mathbf{w}_{\Delta}$ and $\mathbf{w}_{\Delta}^{(\mathrm{cnv})}$—are shown in Fig. 4 along with the theoretical angle accuracies of the CRLB in (13) and conventional monopulse in (20). Note that the RMSE in Fig. 4 is normalized by the sum beamwidth. It is observed that the plots of monopulse estimation with the optimum difference taper are in agreement with the CRLB and that the angle accuracy is improved over the conventional monopulse angle accuracy. The quantitative accuracy improvement in the plots is 1.16 on an average, which is in agreement with the theoretical value. From the radar system engineering perspective, the accuracy improvement with the optimum difference taper is equivalent to allocating 1.3 dB of reduced SNR for meeting the requisite angle accuracy. The sum and difference beampatterns for 0°–90° in azimuth and for −10°–10° in azimuth are plotted in Figs. 5 and 6, respectively. From Fig. 5, it is observed that the sum beampattern shows lower sidelobe levels compared with the difference beampatterns. Both difference beampatterns show similar sidelobe roll-offs as seen in the figure, but their peak sidelobe levels are −10.7 dB for the optimum difference beampattern and −13.3 dB for the conventional difference beampattern as observed in Fig. 6. The optimum difference beampattern has a peak sidelobe level degraded by 2.6 dB, but the gains of the dual beams within the sum beamwidth of 1.58° are slightly higher than that of the conventional difference beampatterns. These differences contribute to the angle-accuracy improvement to achieve the CRLB in the optimum difference beampattern.

VI. CONCLUSION

The monopulse angle-estimation technique to achieve the CRLB for angle accuracy was investigated for the DBF radar. The derivation of the monopulse angle accuracy with the optimum difference taper for a fully digitized array radar was presented, and an improvement in the accuracy over the conventional monopulse accuracy was proved theoretically. A suboptimum solution for the optimum difference taper for subarray-based DBF radars was provided. The results of computer simulations with ULA were included to demonstrate the accuracy improvement by a factor of 1.16 (over the conventional monopulse), which was equivalent to a 1.3 dB reduction in the SNR for the requisite angle accuracy in fully digitized array radars.

APPENDIX
DERIVATION OF CRLB FOR A SYMMETRICAL LINEAR ARRAY

For a symmetrical linear array, whose element antenna positions and antenna tapers are given by (10) and (11), the steering vector $\mathbf{a}'(u)$ is expressed as

$$\mathbf{a}'(u) = \begin{bmatrix} \alpha_1 \exp\left(j\frac{2\pi d_1}{\lambda}u\right), \ldots, \alpha_{\frac{M}{2}} \exp\left(j\frac{2\pi d_{\frac{M}{2}}}{\lambda}u\right), \\ \alpha_{\frac{M}{2}} \exp\left(-j\frac{2\pi d_{\frac{M}{2}}}{\lambda}u\right), \ldots, \alpha_1 \exp\left(-j\frac{2\pi d_1}{\lambda}u\right) \end{bmatrix}^T. \quad (44)$$

Thus, $\frac{\partial \mathbf{a}'(u)}{\partial u}$ can be expressed as

$$\frac{\partial \mathbf{a}'(u)}{\partial u} = j\frac{2\pi}{\lambda}\mathbf{D}\mathbf{a}'(u) = \mathbf{a}_{\Delta}{}'(u). \quad (45)$$

It should be noted that $j\frac{2\pi}{\lambda}\mathbf{D}$ in (45) is a taper for forming the difference beam so that $\frac{\partial \mathbf{a}'(u)}{\partial u}$ is denoted as $\mathbf{a}_{\Delta}{}'(u)$. Orthogonality between $\mathbf{a}'(u)$ and $\mathbf{a}_{\Delta}{}'(u)$ holds as $\mathbf{a}'^{H}(u)\mathbf{a}_{\Delta}{}'(u) = 0$.

From (45), the following is true:

$$\mathbf{D}\mathbf{a}(u) = \frac{\lambda}{j2\pi}\mathbf{T}_{SL}{}^{-1}\mathbf{a}_{\Delta}{}'(u). \quad (46)$$

Thus, the terms in (7) are reduced to

$$\mathbf{a}^{H}(u)\mathbf{D}\left(\mathbf{I} - \frac{\mathbf{a}(u)\mathbf{a}^{H}(u)}{\mathbf{a}(u)^{H}\mathbf{a}(u)}\right)\mathbf{D}\mathbf{a}(u) = \mathbf{a}^{H}(u)\mathbf{D}\mathbf{D}\mathbf{a}(u). \quad (47)$$

Finally, (7) is reduced to (12).

REFERENCES

[1] M. Skolnik
Radar Handbook, 3rd ed. Columbus, OH, USA: McGraw-Hill, 2008.

[2] S. M. Sherman and D. K. Barton
Monopulse Principles and Techniques, 2nd ed. Norwood, MA, USA: Artech House, 2011.

[3] U. Nickel
Overview of generalized monopulse estimation
IEEE Aerosp. Electron. Syst. Mag., vol. 21, no. 6, pp. 27–56, Jun. 2006.

[4] A. K. Agrawal and E. L. Holzman
Beamformer architectures for active phased-array radar antennas
IEEE Trans. Antennas Propag., vol. 47, no. 3, pp. 432–442, Mar. 1999.

[5] I. Kanter
The effect of jamming on monopulse accuracy
IEEE Trans. Aerosp. Electron. Syst., vol. AES-15, no. 5, pp. 738–741, Sep. 1979.

[6] F. L. C. Lin and F. F. Kretschmer
Angle measurement in the presence of mainbeam interference
IEEE Aerosp. Electron. Syst. Mag., vol. 5, no. 11, pp. 19–25, Nov. 1990.

[7] W. D. Blair and M. Brandt-Pearce
Monopulse DOA estimation of two unresolved Rayleigh targets
IEEE Trans. Aerosp. Electron. Syst., vol. 37, no. 2, pp. 452–469, Apr. 2001.

[8] D. G. Manolakis, V. K. Ingle, and S. M. Kogan
Statistical and Adaptive Signal Processing: Spectral Estimation, Signal Modeling, Adaptive Filtering and Array Processing. New York, NY, USA: McGraw-Hill, 2000.

[9] J. Ward
Cramer-Rao bounds for target angle and Doppler estimation with space-time adaptive processing radar
In *Proc. Conf. Rec. 29th Asilomar Conf. Signals Syst. Comput.*, 1995, vol. 2, pp. 1198–1202.

[10] A. Dogandzic and A. Nehorai
Cramer-Rao bounds for estimating range, velocity, and direction with an active array
IEEE Trans. Signal Process., vol. 49, no. 6, pp. 1122–1137, Jun. 2001.

[11] R. C. Davis, L. E. Brennan, and L. S. Reed
Angle estimation with adaptive arrays in external noise fields
IEEE Trans. Aerosp. Electron. Syst., vol. AES-12, no.2, pp. 179–186, Mar. 1976.

[12] R. O. Nielsen
Accuracy of angle estimation with monopulse processing using two beams
IEEE Trans. Aerosp. Electron. Syst., vol. 37, no. 4, pp. 1419–1423, Oct. 2001.

[13] R. Takahashi, K. Hirata, T. Hara, and A. Okamura
Derivation of monopulse angle accuracy for phased array radar to achieve Cramer-Rao lower bound
In *Proc. IEEE 37th Int. Conf. Acoust. Speech Signal Process.*, Kyoto, Japan, Mar. 25–30, 2012, pp. 2569–2572.

[14] R. Takahashi, T. Hara, and A. Okamura
Monopulse beamforming to achieve Cramer-Rao lower bound for digital array radar
In *Proc. IEEE Int. Symp. Phased Array Syst. Technol.*, Waltham, MA, USA, 2013, pp. 719–724.

[15] H. L. Van Trees
Optimum Array Processing. New York, NY, USA: Wiley, 2002.

[16] M. A. Richards, J. A. Scheer, and W. A. Holms
Principles of Modern Radar Basic Principles. Raleigh, NC, USA: Scitech Publishing, Inc., 2010.

[17] E. Brookner
Practical Phased Array Antenna Systems. Norwood, MA, USA: Artech House, 1991.

[18] E. T. Bayliss
Designs of monopulse antenna difference patterns with low sidelobes
Bell Syst. Tech. J., vol. 47, pp. 623–650, May/Jun. 1968.

Ryuhei Takahashi (M’12) received the B.S. degree in electrical engineering from the Tokyo Science University, Tokyo, Japan, in 1993. He is currently toward the Ph.D. degree in engineering at the University of Electro-Communications, Chofu, Japan, under the guidance of Prof. Dr. Takayuki Inaba.

Since 1993, he has been with the Kamakura works of Mitsubishi Electric Corporation, Kamakura, Japan, as a radar system Engineer mainly developing ground-based and shipboard active phased array radar systems. In addition to developing these radar systems, from 1993 to 1998, he worked on developing the signal processing algorithm for an experimental airborne magnetic sensing system. Since 2007, he has been with the Information Technology R&D Center of the corporation, researching a wide range of radar signal processing techniques.

Mr. Takahashi is a member of IEICE.

Takayuki Inaba (M’05–SM’07) received the B.S. degree in the Department of Physics, the M.E. degree in physics, and the Ph.D. degree in engineering from the Tokyo Institute of Technology, Tokyo, Japan, in 1981, 1983, and 2001, respectively.

Since April 2008, he has been with the University of Electro-Communications, Chofu, Japan, where he is a Professor in the Department of Mechanical and Intelligent Systems Engineering, Graduate School of Informatics and Engineering. He has been engaged in the research and development of radar signal processing, adaptive array signal processing, and automotive radar systems.

Dr. Inaba received the IEEJ Distinguished Paper Award (72nd), the 2014 IEEE AES Japan-Chapter Best Paper Award, the 2009 IEICE Communications Society Distinguished Contributions Award, the 2007 IEEE AES Japan-Chapter Best Paper Award, and the 2006 IEICE Communications Society Excellent Paper Award.

Toru Takahashi (M'95–SM'04) was born in Kanagawa, Japan, on January 6, 1970. He received the B.E. and M.E. degrees in electrical engineering and the D.E. degree in computer science and engineering from Waseda University, Tokyo, Japan, in 1992, 1994, and 2010, respectively.

In 1994, he joined Mitsubishi Electric Corporation, Kamakura, Japan, where he has been engaged in research and development on antennas for radar and radio communication systems. He is currently the Manager of the Electronics Systems Technology Department, Information Technology R&D Center.

Dr. Takahashi received the Young Engineer Award from the Institute of Electronics, Information and Communication Engineers (IEICE) of Japan in 1999, and the IEICE Communications Society Best Paper Award in 2013. He is a senior member of the IEICE of Japan.

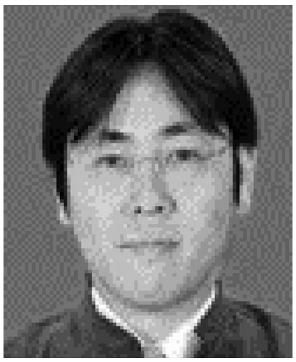

Hirohisa Tasaki received the B.E. and M.E. degrees in electrical engineering from Tokyo Institute of Technology, Tokyo, Japan, in 1985 and 1987, respectively.

In 1987, he joined Mitsubishi Electric Corporation, Kamakura, Japan, where he has been engaged in research and development on speech coding and synthesis. Since 2014, he has been engaged in research and development on radar signal processing. He is currently the General Manager of the Electronics Systems Technology Department, Information Technology R&D Center of the corporation.